



Fluorescent Noble Metal Nanoclusters Loaded Protein Hydrogel Exhibiting Anti-Biofouling and Self-Healing Properties for Electrochemiluminescence Biosensing Applications

Cuiyan Han and Weiwei Guo*

Electrochemiluminescence (ECL) showed great potential in various analytical applications, especially in the sensing of biotargets, taking advantage of its high sensitivity, selectivity, ease of spatial and temporal control, and simplified optical setup. However, during the sensing of complex biological samples, ECL sensors often suffered severe interferences from unavoidable nonspecific-binding of biomacromolecules and physical damages of ECL sensing interfaces. Herein, a hydrogel based ECL biosensing system exhibiting excellent anti-biofouling and self-healing properties is developed. A protein hydrogel composed of bovine serum albumin (BSA) directed fluorescent Au/Ag alloy nanoclusters (Au/Ag NCs) is applied in building ECL sensing systems. The hydrogel matrix facilitates the immobilization of fluorescent Au/Ag NCs as excellent ECL probes, and the porous hydrophilic structure allows the free diffusion of small molecular biotargets while rejecting macromolecular interferences. Moreover, the hydrogel exhibits excellent self-healing property, with the ECL intensity recovered rapidly in 10 min after cutting. The hydrogel ECL system is successfully applied in sensing glutathione (GSH) in serum, confirming the applicability of the hydrogel based anti-biofouling ECL sensing system in sensing complex biological samples. This research may inspire the development of novel anti-biofouling and self-healing ECL biosensors for biosensing applications.

1. Introduction

Taking advantage of the high sensitivity, selectivity, ease of spatial and temporal control, and simplified optical setup, electrochemiluminescence (ECL) method which involves the generation of luminescence signals on an electrode surface through electrochemical processes has emerged as a powerful

analytical method over the past few decades, and holds great promise in various analytical application fields, especially in the analysis of biological samples.^[1–3] By far, remarkable efforts have been made to develop various types of ECL based biosensing systems,^[4,5] and the recent introduction of new ECL materials or mechanisms, such as metal-organic frameworks, aggregation-induced emission luminogens or single atom catalysts, further improved the performance and application ranges of ECL based biosensing systems.^[6–11] However, as a method extremely sensitive to the state of the electrode surface, nonspecific adsorption of biological macromolecules, in particular proteins, and physical scratches of the electrode surfaces, during the sensing of complex biological samples, severely affects the accuracy and practical applicability of the ECL biosensing systems.^[12] In order to meet the requirements of anti-interference and long-term application in practical biosensing applications, it is highly demanded to develop ECL biosensing systems with anti-biofouling and self-healing

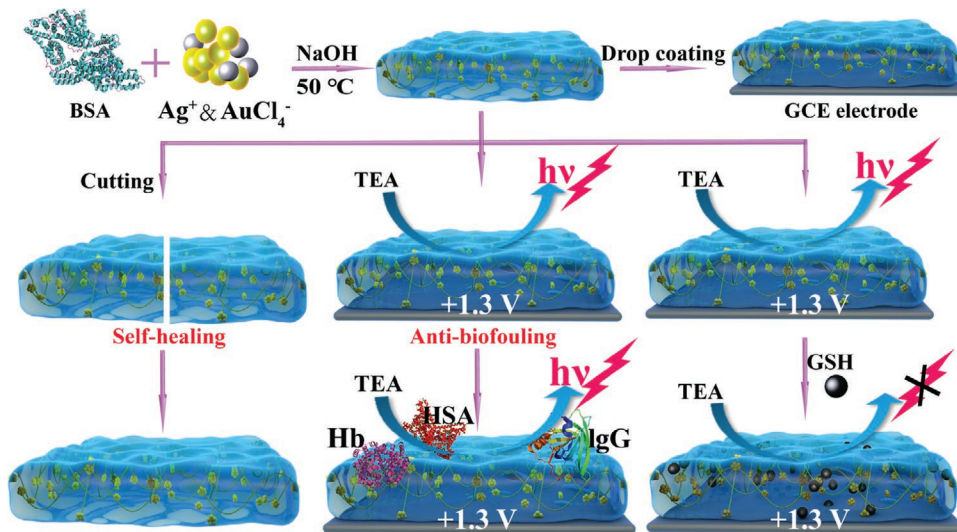
properties. Although some efforts have been made to enhance the anti-biofouling property of ECL biosensing systems, for example, the introduction of hydrophilic polymers or biopolymers to construct protein-resistant anti-fouling electrode surfaces, these methods still encounter the disadvantages such as poor conductivity and complicated synthesis procedures.^[13–15] Furthermore, few studies worked on the development of ECL biosensing system exhibiting self-healing properties, or, even more, ECL sensing systems exhibiting anti-biofouling and self-healing properties simultaneously.^[16] Therefore, the construction of ECL biosensing systems exhibiting both antifouling and self-healing properties is highly desired and of great importance for practical biological applications.

Hydrogels composed of 3D crosslinked hydrophilic polymer networks have gained much attention recently as building materials in the construction of electrochemical and ECL biosensing systems.^[17] The highly porous structure of hydrogels allows the efficient immobilization of ECL probes, and also

C. Y. Han, Prof. W. W. Guo
College of Chemistry
Research Centre for Analytical Sciences
Tianjin Key Laboratory of Biosensing and Molecular Recognition
Nankai University
Tianjin 300071, P. R. China
E-mail: weiweiguo@nankai.edu.cn

The ORCID identification number(s) for the author(s) of this article can be found under <https://doi.org/10.1002/smll.202002621>.

DOI: 10.1002/smll.202002621



Scheme 1. Schematic illustration of the preparation process of Au/Ag NCs@BSA hydrogel possessing self-healing and antifouling properties and Au/Ag NCs@BSA hydrogel-based ECL sensing system for GSH detection.

allows the rapid diffusion of small molecular ECL co-reagents and biotargets.^[18,19] The introduction of conductive polymers or nanostructures into the hydrogel networks can enhance the sensitivity of the systems,^[20–22] and the introduction of responsive structures can endow the system tunable and responsive ECL properties.^[23,24] Furthermore, the high water content, flexibility and good biocompatibility also facilitate the biological application of hydrogel based ECL biosensing systems.^[25] As a unparalleled building material, hydrogel can also be utilized to develop high performance ECL biosensing systems for biological applications, especially the ECL biosensing system exhibiting anti-biofouling and self-healing properties. The porous structure of hydrogel matrix can prevent macromolecular substances, such as proteins, from contacting and contaminating the electrode surface, and, by introducing non-covalent crosslinking mechanisms, such as hydrogen bonding, hydrophobic interaction, electrostatic interaction or physical entanglement of polymer chains, the hydrogel can exhibit self-healing properties.^[16,17] Therefore, it is highly expected to develop hydrogel based ECL biosensing system that exhibited anti-biofouling and self-healing properties simultaneously. Among the materials that can form hydrogels, proteins with excellent intrinsic biocompatibility can be utilized to fabricate physically crosslinked hydrogels through very simple processes.^[26–29] More interestingly, some proteins or peptides, especially bovine serum albumins (BSA), can serve as efficient templates for the formation of fluorescent noble metal nanoclusters (NCs),^[30–32] and the unique size-dependent optical and electrochemical properties of noble metal NCs due to quantum confinement effect have showed potential in ECL applications as ECL labels.^[33–35]

Herein, we report on the development of a protein hydrogel based ECL biosensing system exhibiting anti-biofouling and self-healing properties. A protein hydrogel composed of gelated BSA and BSA templated Au/Ag alloy nanoclusters (Au/Ag NCs@BSA) was prepared, and applied in the construction of ECL biosensing system, as shown in **Scheme 1**. The Au/Ag NCs in the hydrogel matrix can serve as centers to produce

ECL signals in an electrochemical reaction process in the presence of co-reagent, triethylamine (TEA), and the anti-biofouling performance of the Au/Ag NCs@BSA hydrogel based ECL biosensing system against biomacromolecular pollutions of model proteins was investigated. Moreover, the self-healing property of the Au/Ag NCs@BSA hydrogel as well as the hydrogel based ECL biosensing system was investigated. Furthermore, the applicability of the Au/Ag NCs@BSA hydrogel based ECL biosensing system in complex biological systems was verified by detecting glutathione (GSH) in serum, which is a key indicator for the maintenance of intracellular signal transduction, gene regulation and xenobiotic metabolism,^[36] as a model system.

2. Results and Discussion

Fluorescent Au/Ag NCs@BSA hydrogel was prepared based on a modified method reported recently on *in situ* assembly of fluorescent Au NCs within BSA hydrogel networks,^[32] as it has been demonstrated that the Au/Ag bimetallic NCs exhibited enhanced fluorescence and ECL emissions.^[34] As shown in **Figure 1A,B**, a brown hydrogel bulk which exhibited intense red fluorescence under UV lamp was formed, and the fluorescence spectroscopy study of Au/Ag NCs@BSA hydrogel revealed an excitation and emission maxima at 540 and 620 nm, respectively. It should be noted that the molar ratio of Au/Ag plays a key role on the wavelength and intensity of maximum fluorescent emission of the Au/Ag NCs@BSA hydrogel system, and the fluorescent emission intensity reached maximum at an optimal Au/Ag molar ratio of 6:1 (**Figure S1A,B**, Supporting Information). Oscillatory frequency sweep study revealed that the system exhibited a higher storage modulus (G') value than the loss modulus (G'') over the tested frequency region, confirming the gel state of the system (**Figure 1C**). Scanning electron microscope (SEM) image shown in **Figure 1D** confirmed the formation of a highly porous 3D network structure of the freeze-dried Au/Ag NCs@BSA hydrogel. Energy dispersive

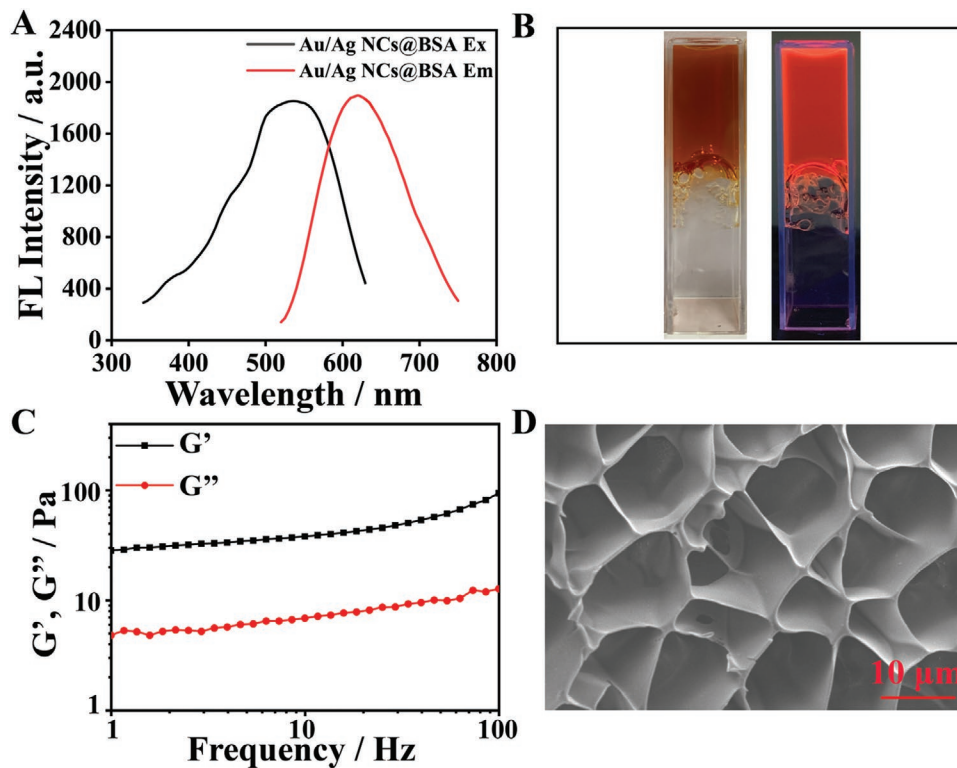


Figure 1. A) Fluorescence excitation (black curve) and emission (red curve) spectra of Au/Ag NCs@BSA hydrogel. B) Photographs of Au/Ag NCs@BSA hydrogel under room light (left) or under 365 nm UV lamp (right), respectively. C) Oscillatory frequency sweep measurement of Au/Ag NCs@BSA hydrogel performed at a fixed strain of 5%. D) SEM image of freeze-dried Au/Ag NCs@BSA hydrogel (Au/Ag molar ratio of 6/1).

spectroscopy (EDS) mapping results revealed a porous network structure of the hydrogel consisted a uniform distribution of N, S, Au, and Ag elements (Figure S2, Supporting Information). X-ray photoelectron spectroscopy (XPS) revealed that the state of gold element of the Au/Ag NCs within BSA hydrogel was dominantly assigned to the Au (0) metallic state with binding energies of 83.9 eV for Au 4f_{7/2} and 87.5 eV for Au 4f_{5/2}, respectively, and the silver element was assigned to the coexistence of Ag (I) and Ag (0) state revealed by the binding energies of 367.7 eV for Ag 3d_{5/2} and 374.2 eV for Ag 3d_{3/2} (Figure S3A–C, Supporting Information).^[37,38] These results confirmed the formation of fluorescent Au/Ag NCs containing BSA hydrogel. Based on some previous reports,^[30,32,39] the formation mechanism of the Au/Ag NCs@BSA hydrogel was proposed as follows: First, the secondary structure of the BSA molecule was disrupted in alkaline condition at 50 °C, which was revealed by the increase of molar ellipticity of BSA molecule after forming the Au/Ag NCs@BSA hydrogel (Figure S3E, Supporting Information).^[40,41] As shown in Table S1 (Supporting Information), during the gelation, the content of α -helix decreased, while the contents of β -fold and random curl increased, which led to the unfolding of BSA molecules and facilitated the crosslinking between unfolded BSA molecules. Infrared spectroscopy combined with Fourier transform (FT-IR) was further applied to study the structure changes of BSA. As shown in Figure S3F (Supporting Information), after forming the Au/Ag NCs@BSA hydrogel, bands at 1516, 1543, and 3291 cm⁻¹ of native BSA were shifted to 1532, 1544, and 3271 cm⁻¹, respectively, confirming

the conformational changes of BSA molecules during the gelation.^[32,34] Meanwhile, AuCl₄⁻ and Ag⁺ ions were reduced by BSA to form the Au/Ag NCs anchoring in the protein scaffold via metal-S binding, as confirmed by the XPS study in which the appearance of peak at 163.2 eV supported the involvement of the S 2p in the metal-S bonding (Figure S3D, Supporting Information), and the formed NCs could function as crosslinking points to promote the crosslinking between BSA molecules and the formation of hydrogel networks.^[32] Finally, after cooling down the reaction solution, a hydrogel composed of crosslinked unfolded BSA molecules and Au/Ag NCs formed.

Fluorescent noble metal NCs had already been demonstrated as excellent ECL probes in the solution phase and modified electrode surface,^[33–42] and the immobilization of these NCs in a hydrophilic hydrogel film that allows the free diffusion of co-reagents and salts would not significantly affect their ECL processes, in which the Au/Ag NC near the electrode surface can be electro-oxidized to form Au/Ag NC⁺ and then react with a reductive radical (TEA[·]) generated from the electro-oxidation and deprotonation of co-reagent TEA, to produce a excited state of the NC and thus emit light (Figure 2A). As expected, intense ECL emission of the Au/Ag NCs@BSA hydrogel film modified GCE was observed during a cyclic voltammetry (CV) scan in the presence of TEA (Figure 2B). It should be noted that the molar ratio of Au/Ag also significantly affect the ECL emision, and a maximum ECL intensity was obtained at a ratio of 6:1, which was also consistent with the fluorescent emission results (Figure S1C, Supporting Information). In a CV study

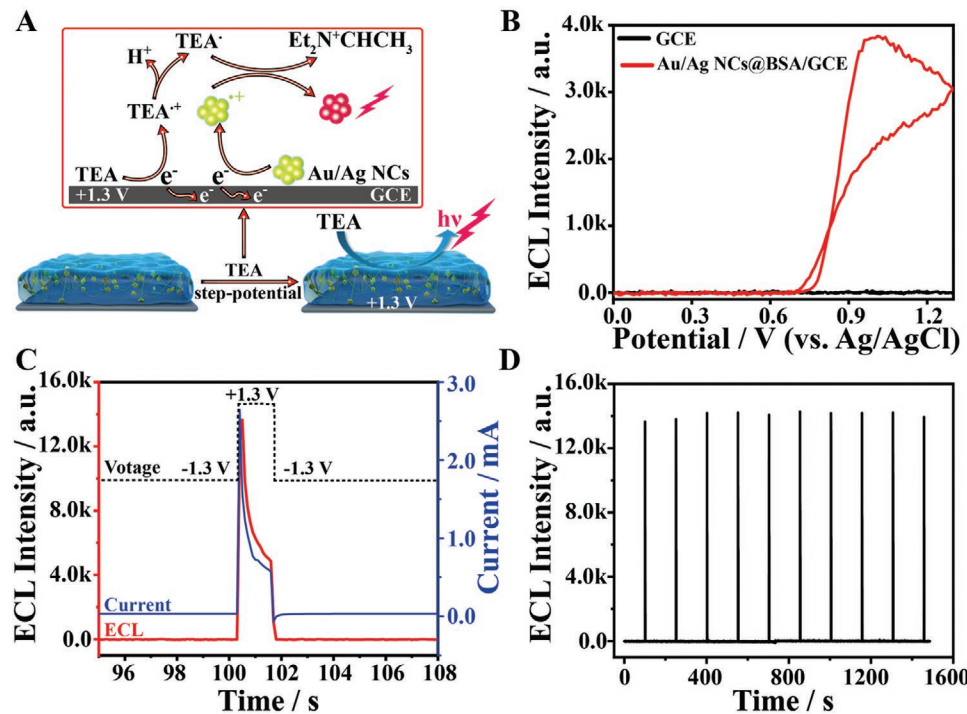


Figure 2. A) Schematic illustration of the mechanism of ECL production of Au/Ag NCs@BSA hydrogel in the presence of TEA by step-potential method. B) ECL intensity as a function of potential of bare GCE (black curve) and Au/Ag NCs@BSA hydrogel modified GCE (red curve) during a cyclic voltammetry scan, respectively (Scan speed, 0.1 V s^{-1}). C) The current versus time curve (blue) and ECL intensity versus time curve (red) of Au/Ag NCs@BSA hydrogel modified GCE during a step-potential from -1.3 to $+1.3\text{ V}$ and back to -1.3 V . D) ECL intensity versus time curves of Au/Ag NCs@BSA hydrogel modified GCE during the potential steps from -1.3 V (100 s) to $+1.3\text{ V}$ (1.3 s) and back to -1.3 V (50 s) for 10 cycles.

of the Au/Ag NCs@BSA hydrogel modified GCE, as shown in Figure S4A,B (Supporting Information), a linear dependence of the peak current with the square root of scan rate ($v^{1/2}$) was observed, indicated that the electrochemical process was mainly controlled by diffusion process rather than adsorption process. As the ECL intensity of the system exhibited a gradually decrease during continuous CV scans (Figure S4C, Supporting Information), due to the incomplete of the diffusion process during scans, a step-potential method coupled with a pre-oxidation process was further applied to investigate the system in order to achieve higher ECL emission and better stability which is crucial for its sensing applications.^[45] As a result, at an optimal step-potential condition (-1.3 to $+1.3\text{ V}$, Figure 2C), the Au/Ag NCs@BSA hydrogel modified GCE exhibited intense and stable ECL emission during consecutive potential scans (Figure 2D), suggesting that the ECL emission of the system is repeatable and stable for sensing applications. To further investigate the influence of the thickness of hydrogel films on the ECL intensity and anti-biofouling performance of the system, hydrogel films with different thickness were formed by drop-casting of different volumes of hydrogels. After a freeze-dry process, SEM results showed that the resultant hydrogel film exhibited a thickness of 80 to 500 μm by drop-casting 1 to 8 μL hydrogel solution, with a good linear relationship between the thickness and hydrogel volume (Figure 3A,B). It is worth noting that the thickness of the hydrogel film has a significant impact on the ECL intensity and anti-biofouling performance of the system (Figure 3C). Results showed that the hydrogel film formed by drop-casting 2 μL hydrogel solution, with the

thickness of $\approx 120\text{ }\mu\text{m}$ measured by SEM, exhibited the highest ECL intensity with excellent anti-biofouling property among the studied films with different thicknesses, implying a film with sufficient thickness helps to generate strong ECL signals and maintain the anti-biofouling property of the system. However, further increasing the film thickness may affect the mass transfer of reactants and products of the ECL reactions and result in a decreased ECL signal. Thus, the optimal hydrogel volume modified on GCE was 2 μL . The effects of pH and temperature on the ECL system were also investigated, and an optimum pH value of 7.4 and optimum operating temperature of 25 °C of the ECL system were obtained (Figure S5, Supporting Information). Under optimal conditions, the as-prepared ECL biosensing system was employed for following experiments.

As a method highly sensitive to the state of the electrode surface, it is still challenging to perform direct ECL detection in biological samples due to the severe biofouling and passivation of electrode surface by the adsorption of biomolecules, especially proteins. In order to evaluate the anti-interference properties of Au/Ag NCs@BSA hydrogel-based ECL system, the ECL response of the system to a wide range of interfering substances, including different proteins and active biomolecules, were investigated, and results showed that no significant quenching effects on the ECL signals were observed in the presence of the interferences except hemoglobin (Hb) showed a slight quenching effect of $\approx 10\%$ (Figure 4A). The good anti-biofouling property of the system was attributed to the porous network structure of hydrogels which allowed the rapid diffusion of small molecular and co-reagents while rejecting the

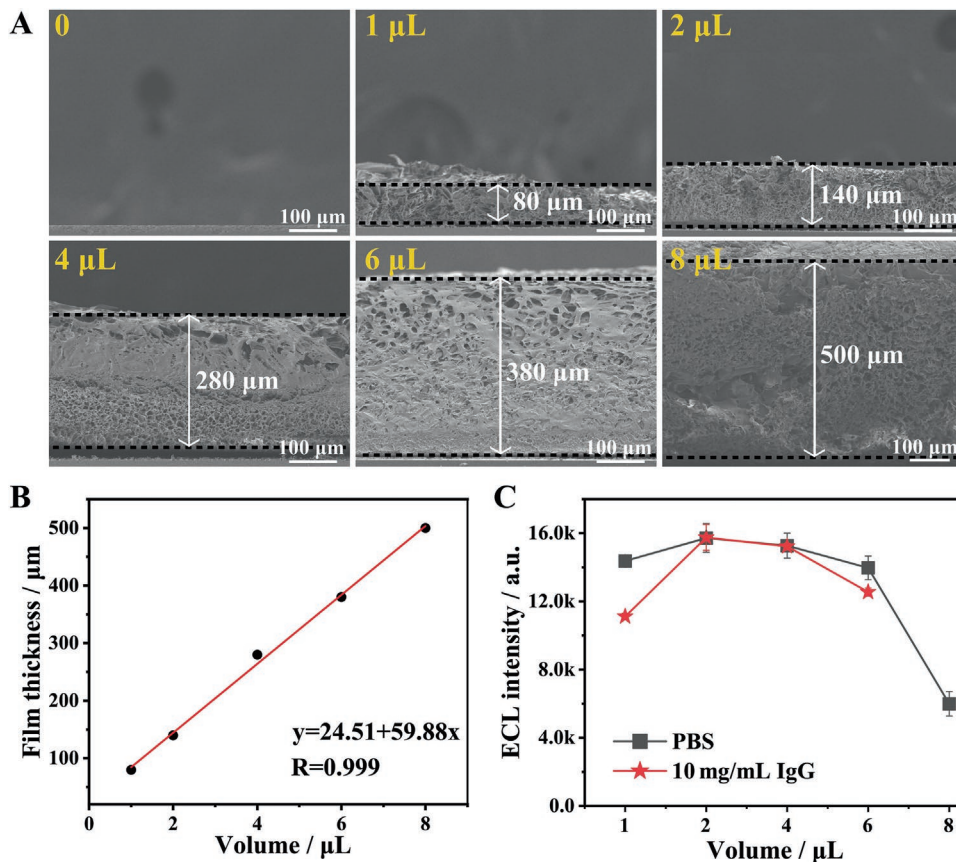


Figure 3. A) SEM images of hydrogel films with different thickness by drop-casting different volumes of hydrogel solutions. B) Linear relationship between film thickness and volume of Au/Ag NCs@BSA hydrogel. C) ECL intensity in blank PBS buffer (the black curve) and ECL intensity in the presence of 10 mg mL^{-1} IgG (the red curve) of the Au/Ag NCs@BSA hydrogel ECL system formed by drop-casting different volumes of hydrogel solutions, with 0.1 M TEA as ECL co-reagents.

approaching of biomacromolecular interferences to passivate the electrode surface (Figure 4B). It should be noted that, although the hydrogel was made of proteins, however, the highly porosity of the hydrogel structure as well as the immobilization of protein molecules within networks greatly reduced the passivation effect by the hydrogel material.

Moreover, physical damages of electrode interfaces during applications is another issue that severely affects the long-term application of ECL based sensing systems, and using materials exhibiting self-healing properties might greatly improve the stability of the ECL system for long-term applications. As shown in Figure 4C, the as-prepared Au/Ag NCs@BSA hydrogel exhibited a self-healing property in cutting experiments, in which the contact of two freshly cut hydrogel pieces could heal the cut surface spontaneously and the resulting hydrogel block could withstand a large strain of stretch by 50%. Step-strain measurement revealed that the hydrogel transformed to a liquid state with higher G'' value than G' upon applying a larger strain of 2000%, and the removal of the larger strain enabled the returning of the hydrogel state with higher G' value than G'' , indicating the self-healing property of the system, as shown in Figure 4D. Furthermore, the effects of hydrogel damage and self-healing on the ECL emission of the system were investigated (Figure 4E). As a result, the ECL intensity of the system immediately decreased

by 17% resulting from the cutting of the hydrogel surface, then the ECL emission of the system started to increase, and almost totally restored to the initial state in 10 min, implied the self-healing of the hydrogel matrix also restored the ECL response of the system. The self-healing property of the hydrogel was attributed to the dynamic character of the thiolate-Au/Ag NCs interaction within the hydrogel as well as the physical crosslinking between protein molecules,^[46–49] and therefore, the dynamically crosslinked network triggered the self-healing of two freshly split hydrogel pieces, as illustrated in Figure 4F. Thus, the Au/Ag NCs@BSA hydrogel ECL system exhibited anti-biofouling and self-healing properties could be applied in the biosensing of complex biological samples.

To validate the utility of the Au/Ag NCs@BSA hydrogel-based ECL system in the sensing of complex biological samples, the sensing of GSH in serum which is a key risk indicator for many diseases including cancers, Alzheimer's disease, and others,^[50] was chosen as a model system. As shown in Figure 5A, the ECL intensity of Au/Ag NCs@BSA based ECL system decreased gradually with the increase of GSH concentrations. The derived calibration plot revealed a linear relationship between ΔECL signals ($\Delta\text{ECL} = I_0 - I$) and GSH concentration in the concentration range of 20 to $200 \times 10^{-6} \text{ M}$ with a correlation coefficient of 0.982, and a detection limit down to $8.7 \times 10^{-6} \text{ M}$ was

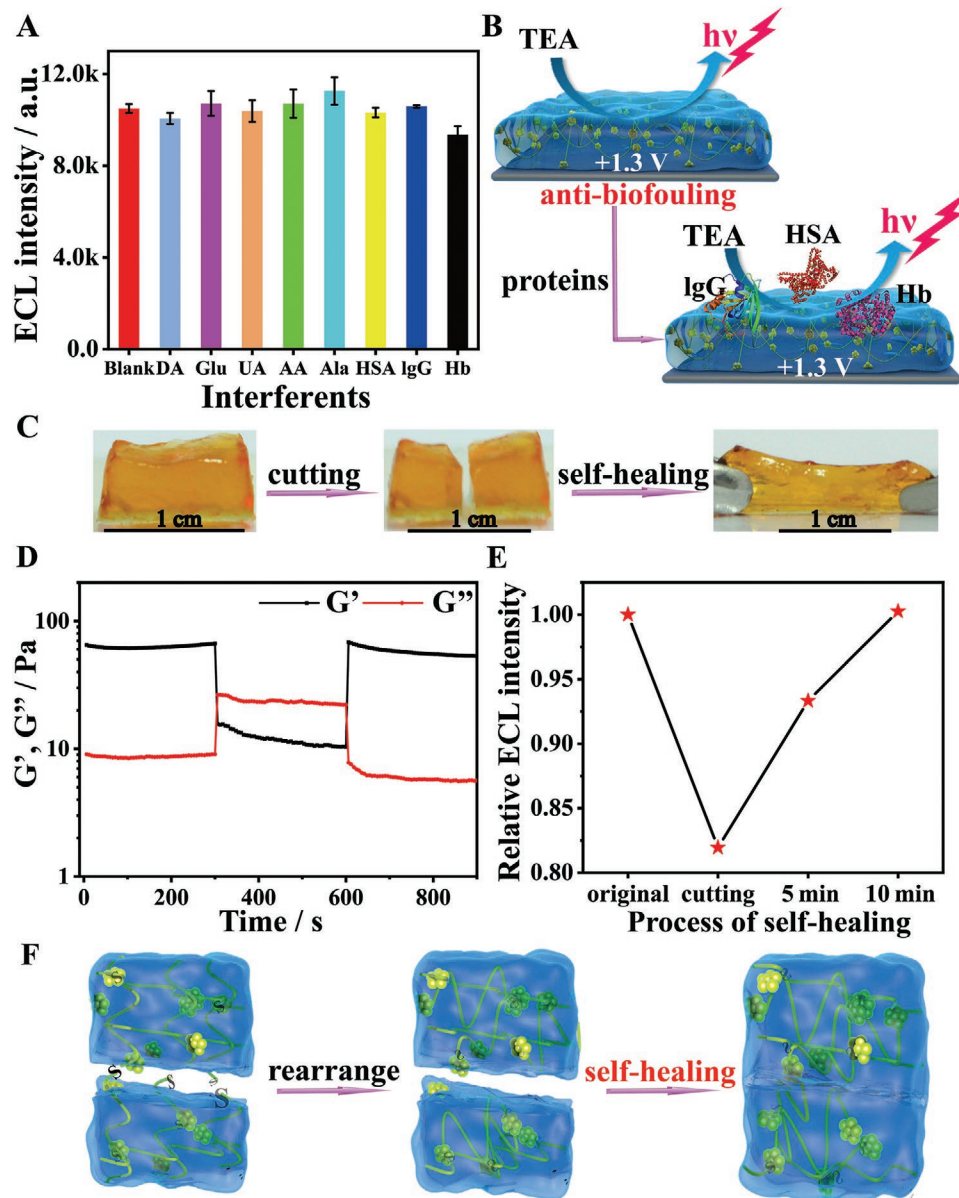


Figure 4. A) ECL intensity of Au/Ag NCs@BSA hydrogel based ECL system in the presence of different interferences. B) Schematic illustration of the anti-biofouling mechanism of Au/Ag NCs@BSA hydrogel based ECL biosensing system. C) Photographs representing the self-healing behavior of a piece of Au/Ag NCs@BSA hydrogel during a process including cutting a hydrogel sample into two pieces, attaching the two hydrogel pieces to allow the self-healing occur, and stretching the healed hydrogel sample. D) The three-step oscillatory time sweep performed by alternating strain from 5% to 2000% and back to 5% with a fixed frequency of 1 Hz. E) The recovery study of the ECL intensity of Au/Ag NCs@BSA hydrogel based ECL system after cutting. F) Schematic illustration of the self-healing mechanism of Au/Ag NCs@BSA hydrogel.

obtained based on $3\delta/\text{slope}$ (Figure 5B). It is worth noting that the ECL emission of the system quenched in the presence of $1200 \times 10^{-6} \text{ M}$ GSH could be restored to 93% after removing the GSH, as shown in Figure 5C, implied the reusability of the hydrogel based ECL sensing system. Moreover, the ECL system showed excellent stability as the ECL intensity remained almost unchanged after 25 days (Figure 5D), which suggests the system is promising for long-term applications. The proposed ECL quenching mechanism by GSH was illustrated in Figure 5E. As a common antioxidant and scavenger of free radicals, the sulphydryl groups of GSH could react with TEA^+ radicals

produced from electro-oxidation of TEA, and therefore inhibited the ECL process between TEA^+ radicals and Au/Ag NCs, which resulted in the quenching of ECL emission.^[33,51] Control experiments showed that the fluorescence emission of the Au/Ag NCs@BSA hydrogel was not affected after being immersed in a solution containing $100 \times 10^{-3} \text{ M}$ GSH for 10 h (Figure S6, Supporting Information), which further clarified that the ECL quenching mechanism was the result of the competitive reaction of GSH and TEA^+ rather than the possible quenching caused by the combination of GSH and metal clusters. The feasibility of the Au/Ag NCs@BSA hydrogel ECL system in the

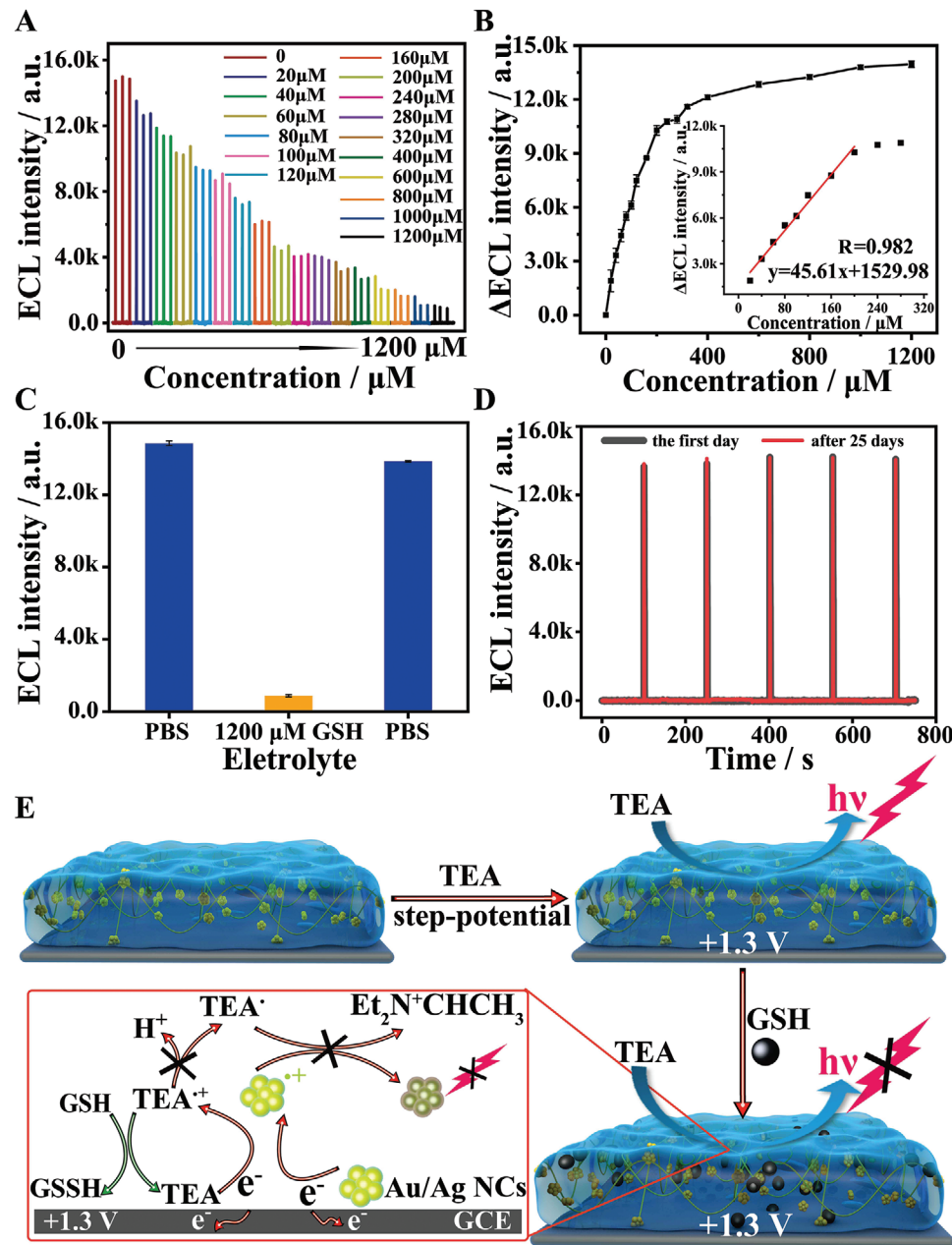


Figure 5. A) ECL intensity of Au/Ag NCs@BSA hydrogel-based sensing system in the presence of GSH with different concentrations. B) The corresponding calibration plot representing the ΔECL ($I_0 - I$) as a function of GSH concentration (inset, linear relationship between the ΔECL intensity and the concentration of GSH). C) ECL intensity of the Au/Ag NCs@BSA hydrogel ECL system responded to PBS buffer, to 1200×10^{-6} M GSH, and back to PBS buffer, respectively. D) ECL intensity of the system at the first day and after 25 days. E) Schematic illustration of the quenching mechanism of GSH to the ECL emission of Au/Ag NCs@BSA hydrogel.

sensing of complex biological samples was further investigated via the detection of GSH in serum. The Au/Ag NCs@BSA hydrogel based ECL system exhibited good performance with satisfactory recoveries (107.3–116.8%) were obtained by adding different amounts of GSH in the diluted serum samples (Table S2, Supporting Information). The sensing system was further compared with other reported GSH sensing methods, with the results shown in Table S3 (Supporting Information). Although the proposed method shows a moderate sensitivity, however, its detection limit is still much lower than the requirements for

detecting GSH concentrations in blood and serum samples. Moreover, the self-healing and anti-biofouling properties of the proposed sensing system may facilitate their long-term sensing applications in complex biological systems.

3. Conclusion

In summary, a hydrogel based ECL system was successfully developed. The Au/Ag NCs@BSA hydrogel showed excellent

and stable ECL performance in the presence of co-reagent TEA. The hydrogel based ECL sensing system exhibited excellent anti-biofouling and self-healing properties may greatly facilitate the future long-term practical sensing applications in complex biological samples. As a model system, the Au/Ag NCs@BSA hydrogel-based ECL system was successfully applied in the label-free detection of GSH in serum. Taking advantage of the facile, rapid and low-cost synthesis method, the hydrogel ECL system may inspire the future development of anti-fouling and self-healing ECL biosensing system for disease diagnosis and wearable biosensing devices.

4. Experimental Section

Materials: Tetrachloroauric (III) acid trihydrate ($\text{HAuCl}_4 \cdot 3\text{H}_2\text{O}$, 99%) was purchased from Sam Chemical Technology Co. Ltd. (Shanghai). Human serum protein (HSA), dopamine (DA), glucose (Glu), uric acid (UA), ascorbic acid (AA), alanine (Ala), and silver nitrate (99.9%) were purchased from Sigma-Aldrich Co. Ltd. (USA). Sodium hydroxide was purchased from Macklin Biochemical Co. Ltd. (Shanghai, China). Triethylamine (TEA, 99.0%) was obtained from TCI Co. Ltd. (Shanghai, China). Glutathione (Reduced) (GSH), Bovine serum albumin (BSA), NaClO_4 (99%), $\text{NaH}_2\text{PO}_4 \cdot 2\text{H}_2\text{O}$, Na_2HPO_4 and KCl were purchased from Aladdin (Shanghai, China). Immunoglobulin (IgG) and hemoglobin (Hb) were purchased from Beijing Solarbio Science Technology Co., Ltd. Human serum samples were purchased from Beijing Solarbio Science Technology Co., Ltd. All of the chemicals were at least of analytical grade, and the water used throughout all experiments was purified by a Milli-Q system (Millipore, Bedford, MA, USA).

Characterization: SEM images were taken with a JSM-7500F scanning electron microscope under 0.1–30 kV accelerating voltage. High-resolution transmission electron microscope (HR-TEM) was performed using a FEI Talos F200x G2 microscope operated at 200 kV. X-ray photoelectron spectroscopy (XPS) spectra were collected by using an Axis Ultra DLD instrument (Kratos Analytical Ltd.) equipped with Al $K\alpha$ radiation. Fluorescence spectra were collected by an F-4600 fluorescence spectrophotometer (HITACHI), with the excitation slit width of 5.0 nm and emission slit width 10.0 nm. Rheological tests were performed using a DHR-2 rheometer (TA Instruments) equipped with a 20 mm parallel-plate geometry with a gap size of 0.2 mm. Circular dichroism (CD) measurements were carried out with a J-715 spectropolarimeter (Jasco, Japan). All electrochemical measurements were carried out with a CHI 660E electrochemical station (Shanghai CH Instrument Co., China). ECL signals were detected by an RFAS-1 automatic electrochemical luminescence spectrophotometer (Xi'an Remex Electronics Co. Ltd.) with the photomultiplier tube (PMT) biased at 1000 V. The three-electrode electrochemical system consisted of an Au/Ag NCs@BSA hydrogel modified glassy carbon electrode (GCE, $\Phi = 3$ mm) as the working electrode, a Pt wire as the auxiliary electrode, and an Ag/AgCl (saturated with KCl) electrode as the reference electrode.

Preparation of Au/Ag NCs@BSA Hydrogel and Au/Ag NCs@BSA Hydrogel Based ECL System: Au/Ag NCs@BSA hydrogels were synthesized based on a modified method reported previously.^[32] In a typical synthesis process, 2 mL mixture solution of BSA (200 mg mL^{-1}) and HAuCl_4 (27×10^{-3} M) was added to a polystyrene cuvette under vigorous stirring. AgNO_3 with different molar ratio to HAuCl_4 was further added to the mixture solution. After 5 min, NaOH was added to adjust the pH value of the mixture solution to 13. The mixture solution was incubated at 50 °C for 3 h to allow the formation of Au/Ag NCs, as indicated by the color change from light yellow to deep brown, and then the resulting solution was cooled to 4 °C to allow the formation of Au/Ag NCs@BSA hydrogel. 2 μL of freshly prepared Au/Ag NCs@BSA liquid at 50 °C was drop-casted to the surface of GCE and then cooled to 4 °C to form the Au/Ag NCs@BSA hydrogel modified GCE which was further applied in ECL applications.

Application of the Au/Ag NCs@BSA Hydrogel Based ECL Sensing System in GSH Detection: First, the Au/Ag NCs@BSA hydrogel modified GCE was immersed in PBS buffer solution (0.1 M, pH 7.0, containing 0.1 M TEA) for 30 min to reach an equilibrium swelling state of the hydrogel matrix, and then the resulting electrode was placed in a three-electrode electrochemical system as the working electrode. Before testing, a pre-oxidation procedure was applied to the ECL sensing system by using an oxidation voltage of +1.3 V for 50 s.^[45] Then, the ECL signals of the sensor in a buffer solution containing different concentrations of GSH were recorded during the potential steps between -1.3 and +1.3 V. Each sample was measured at least three times, and ΔECL ($\Delta\text{ECL} = I_0 - I$, where I_0 is the ECL signal of the system in the absence of GSH, and I is the signal in the presence of different concentrations of GSH) as a function of the GSH concentration was used to plot the calibration curve. In the selectivity test of the ECL sensing system, instead of GSH, 40×10^{-6} M of DA or 200×10^{-6} M of Glu, UA, AA, Ala, were introduced to the ECL sensing system, respectively. In the anti-biofouling test of the system, 10 mg mL^{-1} of HSA, IgG or Hb was added to the ECL sensing system, respectively. To verify the applicability of the ECL sensing system in complex conditions, a mimic actual sample by adding GSH to human serum was prepared. The human serum sample was directly added to the three-electrode electrochemical system containing 0.1 M PBS (pH 7.0) and 0.1 M TEA.

Supporting Information

Supporting Information is available from the Wiley Online Library or from the author.

Acknowledgements

This work was financially supported by the National Natural Science Foundation of China (Grant Nos. 21505078 and 21874076), the Natural Science Foundation of Tianjin City (Grant No. 18JCZDJC37800), the Fundamental Research Funds for Central Universities (China) and the National Program for Support of Top-notch Young Professionals.

Conflict of Interest

The authors declare no conflict of interest.

Keywords

antifouling properties, biosensors, electrogenerated chemiluminescence, fluorescent nanoclusters, protein hydrogels

Received: April 26, 2020

Revised: August 22, 2020

Published online:

- [1] H. D. Abruna, A. J. Bard, *J. Am. Chem. Soc.* **1982**, *104*, 2641.
- [2] M. M. Richter, *Chem. Rev.* **2004**, *104*, 3003.
- [3] W. Miao, *Chem. Rev.* **2008**, *108*, 2506.
- [4] L. L. Li, Y. Chen, J. J. Zhu, *Anal. Chem.* **2017**, *89*, 358.
- [5] C. Ma, Y. Cao, X. Gou, J. J. Zhu, *Anal. Chem.* **2020**, *92*, 431.
- [6] Z. Han, Z. Yang, H. Sun, Y. Xu, X. Ma, D. Shan, J. Chen, S. Huo, Z. Zhang, P. Du, X. Q. Lu, *Angew. Chem., Int. Ed.* **2019**, *131*, 5976.
- [7] Y. Liu, M. Wang, Y. Nie, Q. Zhang, Q. Ma, *Anal. Chem.* **2019**, *91*, 6250.

- [8] Y. Yang, G. B. Hu, W. B. Liang, L. Y. Yao, W. Huang, R. Yuan, D. R. Xiao, *Nanoscale* **2019**, *11*, 10056.
- [9] L. Yang, B. Zhang, L. Fu, K. Fu, G. Zou, *Angew. Chem., Int. Ed.* **2019**, *131*, 6975.
- [10] Y. Zhao, J. Yu, G. Xu, N. Sojic, G. Loget, *J. Am. Chem. Soc.* **2019**, *141*, 13013.
- [11] W. Gu, H. Wang, L. Jiao, Y. Wu, Y. Chen, L. Hu, J. Gong, D. Du, C. Zhu, *Angew. Chem., Int. Ed.* **2020**, *59*, 3534.
- [12] A. Barfodokht, J. J. Gooding, *Electroanalysis* **2014**, *26*, 1182.
- [13] L. Y. Zhang, D. Li, W. L. Meng, Q. Huang, Y. Su, L. H. Wang, S. P. Song, C. H. Fan, *Biosens. Bioelectron.* **2009**, *25*, 368.
- [14] S. Jiang, Z. Cao, *Adv. Mater.* **2010**, *22*, 920.
- [15] Y. X. Li, L. Wang, C. F. Ding, X. L. Luo, *Biosens. Bioelectron.* **2019**, *142*, 111553.
- [16] S. Liu, W. W. Guo, *Adv. Funct. Mater.* **2018**, *28*, 1800596.
- [17] Dhanjai, A. Sinha, P. K. Kalambate, S. M. Mugo, P. Kamau, J. P. Chen, R. Jain, *TrAC, Trends Anal. Chem.* **2019**, *118*, 488.
- [18] G. F. Gui, Y. Zhuo, Y. -Q. Chai, Y. Xiang, R. Yuan, *Biosens. Bioelectron.* **2016**, *77*, 7.
- [19] H. Jiang, Z. Qin, Y. Zheng, L. Liu, X. Wang, *Small* **2019**, *15*, 1901170.
- [20] X. Y. Jiang, H. J. Wang, R. Yuan, Y. Q. Chai, *Anal. Chem.* **2018**, *90*, 8462.
- [21] N. Hao, X. Zhang, Z. Zhou, R. Hua, Y. Zhang, Q. Liu, J. Qian, H. Li, K. Wang, *Biosens. Bioelectron.* **2017**, *97*, 377.
- [22] G. Liu, C. Ma, B. K. Jin, Z. X. Chen, F. L. Cheng, J. J. Zhu, *Anal. Chem.* **2019**, *91*, 3021.
- [23] H. Li, M. Sentic, V. Ravaine, N. Sojic, *Phys. Chem. Chem. Phys.* **2016**, *18*, 32697.
- [24] H. Li, S. Voci, V. r. Ravaine, N. Sojic, *J. Phys. Chem. Lett.* **2018**, *9*, 340.
- [25] C. F. Ding, Y. X. Li, L. Wang, X. L. Luo, *Anal. Chem.* **2019**, *91*, 983.
- [26] Y. L. Li, J. Rodrigues, H. Tomas, *Chem. Soc. Rev.* **2012**, *41*, 2193.
- [27] H. Li, N. Kong, B. Laver, J. Liu, *Small* **2016**, *12*, 973.
- [28] N. Kong, Q. Peng, H. Li, *Adv. Funct. Mater.* **2014**, *24*, 7310.
- [29] J. Kopeček, J. Yang, *Angew. Chem., Int. Ed.* **2012**, *51*, 7396.
- [30] J. Xie, Y. Zheng, J. Y. Ying, *J. Am. Chem. Soc.* **2009**, *131*, 888.
- [31] B. Adhikari, A. Banerjee, *Chem. - Eur. J.* **2010**, *16*, 13698.
- [32] L. Wang, X. Jiang, M. Zhang, M. Yang, Y. N. Liu, *Chem. - Asian J.* **2017**, *12*, 2374.
- [33] Y. M. Fang, J. Song, J. Li, Y. W. Wang, H. H. Yang, J. J. Sun, G. N. Chen, *Chem. Commun.* **2011**, *47*, 2369.
- [34] Q. Zhai, H. Xing, X. Zhang, J. Li, E. Wang, *Anal. Chem.* **2017**, *89*, 7788.
- [35] Y. Zhou, Y. Chai, R. Yuan, *Anal. Chem.* **2019**, *91*, 14618.
- [36] A. Meister, *J. Biol. Chem.* **1988**, *263*, 17205.
- [37] N. Zhang, Y. Si, Z. Sun, L. Chen, R. Li, Y. Qiao, H. Wang, *Anal. Chem.* **2014**, *86*, 11714.
- [38] J. Sun, H. Wu, Y. Jin, *Nanoscale* **2014**, *6*, 5449.
- [39] J. S. Mohanty, P. L. Xavier, K. Chaudhari, M. Bootharaju, N. Goswami, S. Pal, T. Pradeep, *Nanoscale* **2012**, *4*, 4255.
- [40] N. Wangoo, C. R. Suri, G. Shekhawat, *Appl. Phys. Lett.* **2008**, *92*, 133104.
- [41] A. S. Patel, T. Mohanty, *J. Mater. Sci.* **2014**, *49*, 2136.
- [42] L. Li, H. Liu, Y. Shen, J. Zhang, J.-J. Zhu, *Anal. Chem.* **2011**, *83*, 661.
- [43] I. Díez, M. Pusa, S. Kulmala, H. Jiang, A. Walther, A. S. Goldmann, A. H. Müller, O. Ikkala, R. H. Ras, *Angew. Chem., Int. Ed.* **2009**, *48*, 2122.
- [44] A. Chen, S. Ma, Y. Zhuo, Y. Chai, R. Yuan, *Anal. Chem.* **2016**, *88*, 3203.
- [45] H. Peng, Z. Huang, Y. Sheng, X. Zhang, H. Deng, W. Chen, J. Liu, *Angew. Chem., Int. Ed.* **2019**, *58*, 11691.
- [46] J. Zhang, J. Malicka, I. Gryczynski, J. R. Lakowicz, *J. Phys. Chem. B* **2005**, *109*, 7643.
- [47] R. Martín, A. Rekondo, J. Echeberria, G. Cabañero, H. J. Grande, I. Odriozola, *Chem. Commun.* **2012**, *48*, 8255.
- [48] D. Jiang, Q. Xue, Z. Liu, J. Han, X. Wu, *New J. Chem.* **2017**, *41*, 271.
- [49] Y. Song, T. Huang, R. W. Murray, *J. Am. Chem. Soc.* **2003**, *125*, 11694.
- [50] D. Giustarini, I. Dalle-Donne, D. Tsikas, R. Rossi, *Crit. Rev. Clin. Lab. Sci.* **2009**, *46*, 241.
- [51] H. P. Peng, M. L. Jian, Z. N. Huang, W. J. Wang, H. H. Deng, W. H. Wu, A. L. Liu, X. H. Xia, W. Chen, *Biosens. Bioelectron.* **2018**, *105*, 71.